Multiplexed Analysis of Genes Using Nucleic Acid-Stabilized Silver-Nanocluster Quantum Dots

Natalie Enkin, Fuan Wang, Etery Sharon, H. Bauke Albada, and Itamar Willner*

Institute of Chemistry, The Center for Nanoscience and Nanotechnology, The Hebrew University of Jerusalem, Jerusalem 91904, Israel

ABSTRACT Luminescent nucleic acid-stabilized Ag nanoclusters (Ag NCs) are applied for the optical detection of DNA and for the multiplexed analysis of genes. Two different sensing modules including Ag NCs as luminescence labels are described. One sensing module involves the assembly of a three-component sensing module composed of a nucleic acid-stabilized Ag NC and a quencher-modified nucleic acid hybridized with a nucleic acid scaffold that is complementary to the target DNA. The luminescence of the Ag NCs is quenched in the sensing module nanostructure. The strand displacement of the scaffold by the target DNA separates the nucleic acid-functionalized Ag NCs, leading to the turned-on luminescence of the NCs and to the optical readout of the sensing process. By implementing two different-sized Ag NC-modified sensing modules, the parallel multiplexed analysis of two genes (the Werner Syndrome gene and the HIV, human immunodeficiency, gene), using 615 and 560 nm luminescent Ag NCs, is demonstrated. The second sensing module includes the nucleic acid functionalized Ag NCs and the quencher-modified nucleic acid hybridized with a hairpin DNA scaffold. The luminescence of the Ag NCs is quenched in the sensing module. Opening of the hairpin by the target DNA triggers the luminescence of the Ag NCs, due to the spatial separation of the Ag NCs/quencher units. The system is applied for the optical detection of the BRAC1 gene. In addition, by implementing two-sized Ag NCs, the multiplexed analysis of two genes by the hairpin sensing module approach is demonstrated.

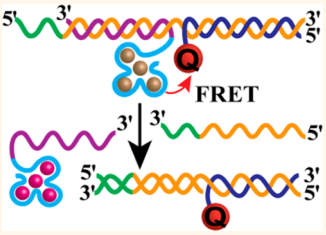

KEYWORDS: sensor · luminescence · optical · gene · nanobiotechnology · nanomaterial

The synthesis and applications of fluorescent metal nanoclusters (NCs), particularly nucleic acid-stabilized Ag^0 nanoclusters (Ag NCs), have recently attracted substantial research efforts.[1,2] Cytosine-rich nucleic acids are usually used to stabilize the Ag NCs, and the stabilization of the NCs by specific single-stranded nucleic acid sequences, or by sequence-specific duplex nucleic acid configurations, were reported.[3−7] The DNA-stabilized Ag NCs exhibit interesting properties, such as tunable luminescence properties, high luminescence quantum yields, good photostability, solubility in aqueous media, biocompatibility, and low cytotoxicity.[8,9] Specifically, the tunable luminescence properties of the Ag NCs were found to be controlled by the size of the Ag NCs and by the specific sequences that stabilize the NCs. Not surprisingly, the unique optical properties of the DNA-stabilized Ag NCs were, recently, implemented to develop different optical sensing platforms[10] and for bioimaging.[11,12] For example, DNA-stabilized Ag NCs were applied for the detection of metal ions such as Hg^{2+} or Cu^{2+},[13] for the analysis of bioactive thiols[14] such as cysteine, homocysteine, or glutathione, for probing aptamer−substrate complexes,[15−17] such as the aptamer−ATP or aptamer−thrombin complexes, for detection of DNA,[18] single nucleotide mutations,[19,20] and micro RNAs,[21] and for probing the activity of enzymes, such as glucose oxidase or tyrosinase.[22] Furthermore, similar to the use of the size-controlled tunable luminescence properties of semiconductor quantum dots for multiplexed analysis of antigens,[23] DNA,[24−26] or aptamer−substrate complexes,[27] the tunable luminescence spectra of Ag NCs were also applied for the multiplexed detection of pathogens or aptamer−substrate complexes.[18] For example, different-sized Ag NCs, exhibiting different luminescence properties, were coupled to DNA probes consisting of the recognition sequences corresponding to the hepatitis B virus (HBV) and of the human immunodeficiency virus (HIV) genes, respectively. The resulting DNA−Ag NCs were adsorbed on graphene oxide, where the luminescence of the Ag NCs was quenched. By the selective desorption of the

* Address correspondence to willnea@vms.huji.ac.il.

Received for review September 3, 2014 and accepted October 19, 2014.

Published online October 19, 2014
10.1021/nn504983j

respective Ag NCs conjugates through the formation of the duplex DNA structures with the target genes, the luminescence of the respective Ag NCs was switched-"ON", thus allowing the multiplexed analysis of the genes. In the present study, we introduce two new sensing configurations that implement Ag NCs for the optical detection and multiplexed analysis of genes. The systems lead to the switched-"ON" luminescent detection of the analytes and the multiplexed analysis of genes using two different-sized Ag NCs. Most importantly, we describe a modular hairpin-based sensing platform that includes versatile quencher-modified nucleic acids and versatile nucleic acid stabilized Ag NCs that allow the sensing and multiplexed sensing of any gene by the appropriate programming of the sensing hairpin probe.

RESULTS AND DISCUSSION

Figure 1A depicts the concept of one sensor configuration that applies Ag NCs as the optical label. We made use of 560 and 615 nm luminescent Ag NCs. The sizes and composition of the Ag NCs were determined by TEM and ESI-mass spectrometry. Figure S1, Supporting Information, exemplifies the TEM image of the 615 nm Ag NCs. The dimension of the clusters is 5−6 nm. It is difficult to distinguish the size differences between the two kinds of Ag NCs. The ESI-mass spectrometry analyses of the Ag NCs reveal that the 615 nm luminescent Ag NCs consist of six to seven Ag atoms, whereas the 560 nm luminescent Ag NCs are composed of four to five Ag atoms (see Table S1, Supporting Information). The excitation spectra of the 560 and 615 nm luminescent Ag NCs are provided in Figures S2 and S3, Supporting Information. The system consists of a DNA template (**1**) that is composed of domains I and II and the overhang III. All of these domains are complementary to the DNA analyte **4**. The sensor system also includes the nucleic acid (**2**)-stabilized Ag NCs strand and the BHQ-functionalized nucleic acid (**3**) (where BHQ = Black Hole quencher). The nucleic acid **2** is composed of domain IV, which stabilizes the Ag NCs (in the specific example the 615 nm luminescent Ag NCs, λ_{ex} = 520 nm[28]) and of domain I′ that is complementary to domain I of the template (**1**). Similarly, the BHQ-modified nucleic acid **3** includes the sequence domain II′ that is complementary to domain II of the template **1**. Thus, the sensing module consists of the template **1** to which the **2**-modified Ag NCs and the BHQ-functionalized nucleic acid **3** are hybridized. In the resulting hybrid-sensing module the luminescence of the Ag NCs is quenched by BHQ due to the spatial proximity between the NCs and the BHQ quencher. In the presence of the target DNA **4**, the template DNA is displaced from the sensing module due to the formation of the energetically favored hybrid **1/4**. Note that in the hybrid **1/4**, the DNA analyte yields a duplex with domains I, II, and III of

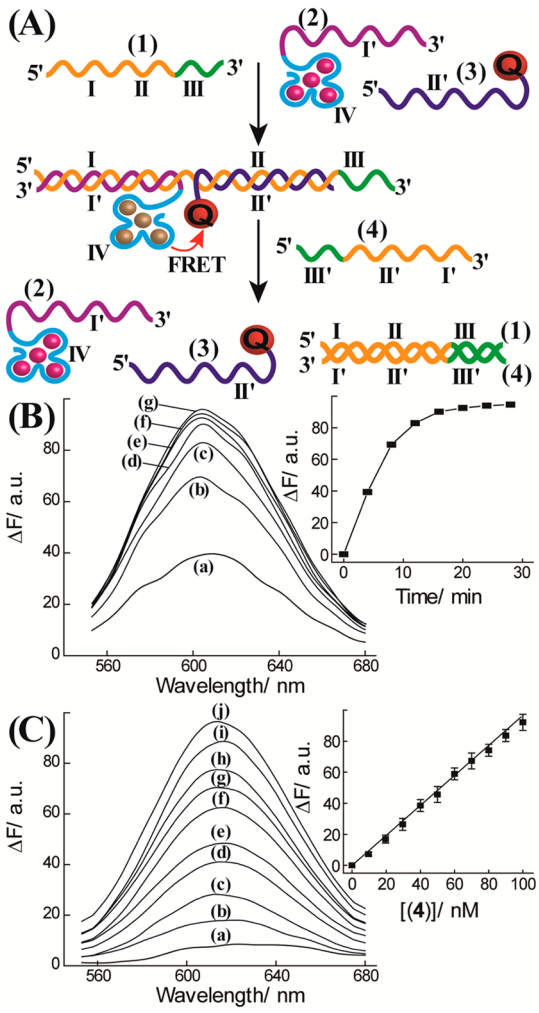

Figure 1. (A) General scheme of the optical detection of a target gene using a sensing module consisting of a probe template, a nucleic acid protected Ag NCs, and a quencher-functionalized nucleic acid. (B) Time-dependent luminescence spectra changes upon subjecting the 1/3/2-modified Ag NCs sensing module to the analyte 4, 1×10^{-7} M: (a) 4, (b) 8, (c) 12, (d) 16, (e) 20, (f) 24, and (g) 28 min. Inset: luminescence changes at λ = 615 nm as a function of time. (C) Luminescence spectra changes (ΔF) observed upon treatment of the sensing module 1/3/2-modified Ag NCs with variable concentrations of target 4 for a fixed time interval of 28 min: (a) 1×10^{-8} M, (b) 2×10^{-8} M, (c) 3×10^{-8} M, (d) 4×10^{-8} M, (e) 5×10^{-8} M, (f) 6×10^{-8} M, (g) 7×10^{-8} M, (h) 8×10^{-8} M, (i) 9×10^{-8} M, and (j) 1×10^{-7} M. Inset: Derived calibration curve corresponding to the luminescence intensity changes of the sensing module at different concentrations of target 4.

the template **1**. As a result, the **2**-stabilized Ag NCs unit and the BHQ-modified **3** unit are separated from the sensing module, leading to the switching-"ON" of the luminescence of the Ag NCs. Figure 1B shows the time-dependent luminescence spectra of the Ag NCs upon treatment of the sensing module with a fixed concentrations of the DNA analyte **4**. The luminescence spectra are intensified with time, and they level-off to a constant value after ca. 28 min, consistent with the separation of the sensing module. Figure 1C depicts the fluorescence spectra of the sensing module upon

treatment with variable concentrations of the DNA analyte **4** for a fixed time interval of ca. 28 min. As the concentration of the analyte increases, the fluorescence of the system intensifies, consistent with the increased separation of the sensing module as the concentration of the analyte is elevated. The inset of Figure 1C shows the derived calibration curve corresponding to the fluorescence changes of the system (ΔF) in the presence of different concentrations of DNA analyte **4**. The system enabled the analysis of target DNA **4** with a detection limit that corresponded to 1 nM.

This general paradigm to use nucleic acid-stabilized Ag NCs as luminescent quantum dots for the detection of DNA was then applied to detect two different genes, the gene associated with the Werner Syndrome and the human immunodeficiency virus (HIV) gene, and to apply two different-sized Ag NCs for the multiplexed analysis of the two genes, Figure 2A. The Werner Syndrome is an autosomal recessive progeroid syndrome which is characterized by the appearance of premature aging.[29−31] The gene associated with this syndrome was identified.[32] To analyze the gene associated with the Werner Syndrome (**7**), we designed a sensor module that consists of the DNA template **5**, that includes the domains I_a, II, and III_a. Domains I_a and II are complementary to the 615 nm luminescent Ag NCs-functionalized nucleic acid **6** and the BHQ-modified nucleic acid **3**, respectively. Domains I_a and III_a are complementary to the Werner Syndrome gene (**7**). As the Werner Syndrome gene displaces the template **5** from the sensor module, the luminescence of the system at 615 nm is switched on. Similarly, the HIV gene (**10**) was analyzed using a sensing module composed of the 560 nm luminescent Ag NCs[33] that are stabilized by the domain V associated with the nucleic acid **9**. For this, the DNA template **8**, that includes the complementary domains I_b and III_b to the HIV gene, was used to assemble the sensing module. The **9**-stabilized Ag NCs (λ_{ex} = 480 nm, luminescence at 560 nm) and the BHQ-functionalized **3** were hybridized with the template unit **8**. Treatment of the hybrid sensing module with the HIV gene (**10**) results in the displacement of the energetically stabilized duplex **8/9** and the separation of the **9**-stabilized Ag NCs. This leads to the turned-on luminescence of the Ag NCs at λ = 560 nm. Figure 2B depicts the fluorescence spectra changes upon analyzing the gene associated with the Werner Syndrome (**7**) according to Figure 2A. Figure S4 (Supporting Information) shows the time-dependent luminescence spectra of the 615 nm luminescent Ag NCs sensing module shown in Figure 2A upon interaction with a fixed concentration of analyte **7**, 1×10^{-7} M. The luminescence spectra increase with time, and they level off to a constant value after ca. 35 min, consistent with the formation of the energetically stabilized duplex **5**/**7** and the separation of the sensing module. The sensing system consisting of 615 nm

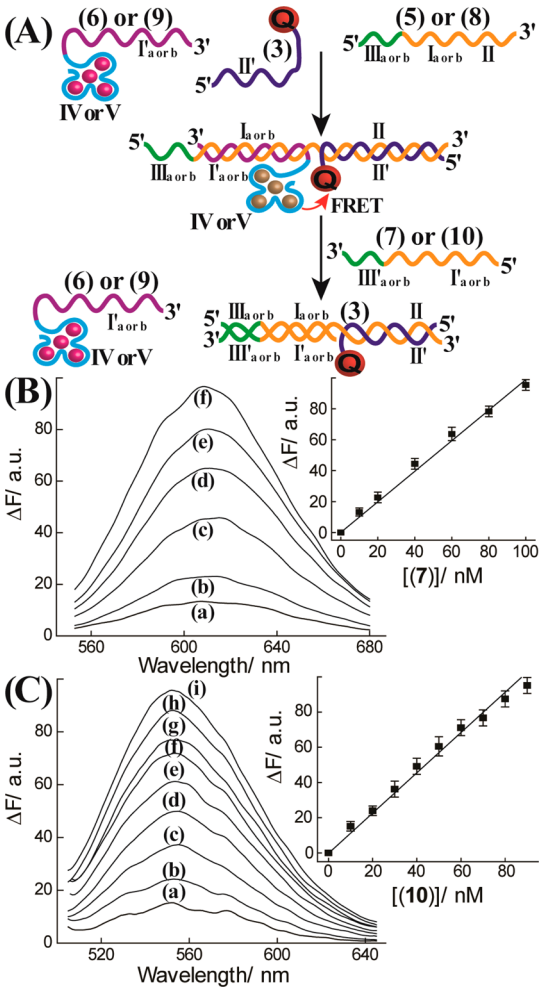

Figure 2. (A) Schematic detection of the Werner Syndrome gene (7) and of the HIV gene (10) using Ag NCs-functionalized sensing modules emitting at 615 and 560 nm, respectively. (B) Luminescence spectra changes observed upon treatment of the 5/3/6-modified Ag NCs sensing module with variable concentrations of the Werner Syndrome gene (7) for a fixed time-interval of 34 min: (a) 1×10^{-8} M, (b) 2×10^{-8} M, (c) 4×10^{-8} M, (d) 6×10^{-8} M, (e) 8×10^{-8} M, and (f) 10×10^{-8} M. Inset: Derived calibration curve corresponding to the luminescence intensity changes (ΔF) of the sensing module at 615 nm in the presence of different concentrations of target 7. (C) Luminescence spectra changes observed upon treatment of the 8/3/9-modified Ag NCs sensing module with different concentrations of the HIV gene (10) for a fixed time-interval of 28 min: (a) 1×10^{-8} M, (b) 2×10^{-8} M, (c) 3×10^{-8} M, (d) 4×10^{-8} M, (e) 5×10^{-8} M, (f) 6×10^{-8} M, (g) 7×10^{-8} M, (h) 8×10^{-8} M, and (i) 9×10^{-8} M. Inset: Derived calibration curve corresponding to the luminescence intensity changes (ΔF) of the system at λ = 560 nm at different concentrations of target 10.

luminescent Ag NCs was then subjected to variable concentrations of target **7** for a fixed time-interval of 34 min. As the concentrations of the analyte gene are elevated, the resulting luminescence changes are intensified, consistent with the increased separation of the sensing module and the generation of higher amounts of the free luminescent Ag NCs. Figure 2B inset depicts the resulting calibration curve corresponding to the luminescence changes of the system

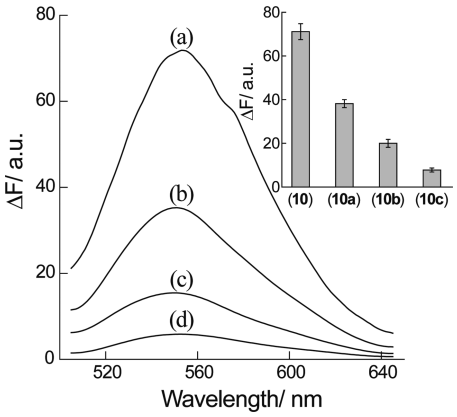

Figure 3. Fluorescence spectra changes upon analysis of 10 and its mutants by the sensing module shown in Figure 2(A): (a) Fluorescence change upon analysis of 10. (b–d) Fluorescence changes upon analyzing one-base, two-base, and three-base mutants 10a, 10b, and 10c, respectively. In all experiments, the concentrations of 3 and 9 are 100 nM, that of 8 is 80 nM, and the concentrations of the analyzed gene/mutants corresponded to 60 nM. All experiments were performed in a mixture of HEPES and phosphate buffer solution, each 10 mM, pH = 7.0, that included $NaNO_3$, 180 mM. Spectra were recorded after a fixed time interval of 28 min.

at different concentrations of DNA analyte **7**. The detection limit for analyzing **7** corresponds to 3 nM. Similarly, the 560 nm luminescent Ag NCs hybrid module shown in Figure 2A was applied to detect the HIV gene (**10**). Figure 2C shows the luminescence spectra changes upon sensing variable concentrations of the HIV gene (**10**) for a fixed time-interval of 28 min. As the concentrations of analyte **10** increase, the luminescence intensities of the system are increased, consistent with the higher degree of separation of the sensing module upon increasing the concentrations of the analyte DNA. The inset of Figure 2 depicts the derived calibration curve. The system enabled the detection of the HIV gene with a detection limit that corresponded to 5 nM. (For the time-dependent luminescence changes of the sensing module upon analyzing a fixed concentration of **10**, that corresponds to 9×10^{-8} M, see Figure S5, Supporting Information).

An important aspect to consider involves the selectivity of the sensing platform and the possibility to detect mutations. This issue was addressed by implementing the sensing scheme shown in Figure 2A to

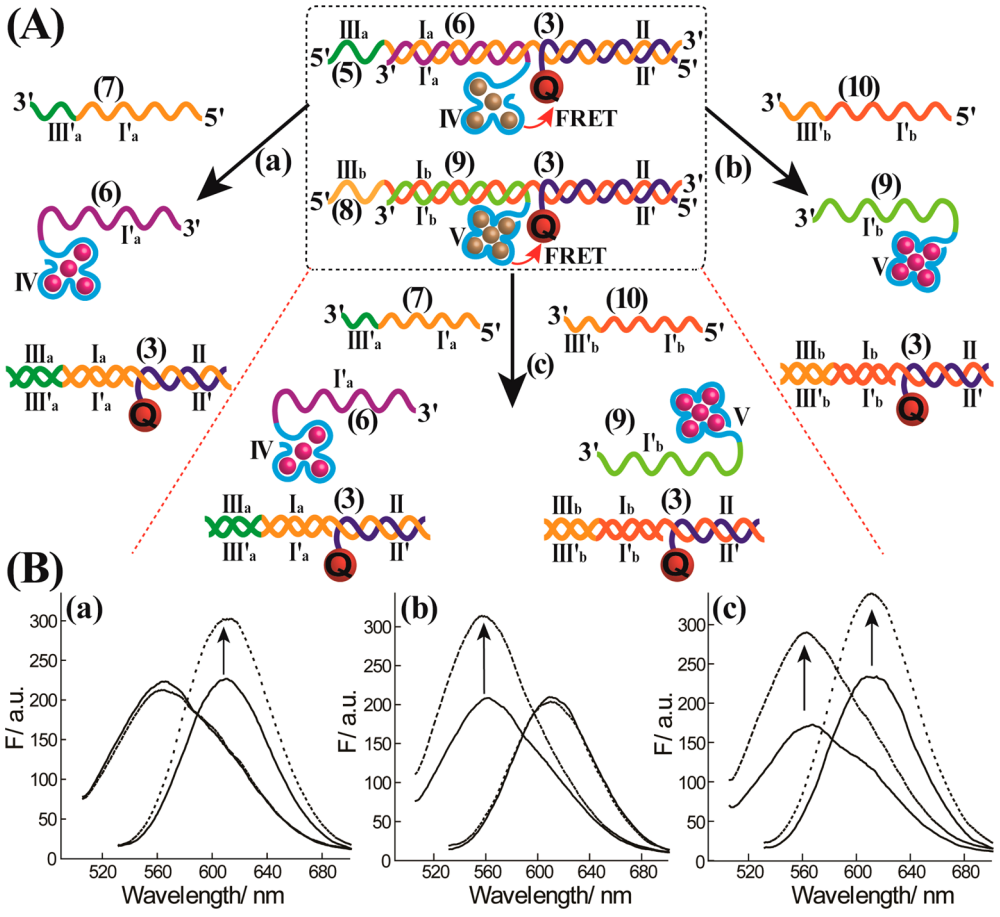

Figure 4. (A) Multiplexed analysis of the Werner Syndrome gene (7) and of the HIV gene (10) using the DNA sensing module composed of the 615 nm luminescent Ag NCs and the 560 nm luminescent Ag NCs. (B) Fluorescence spectra changes upon the multiplexed analysis of the Werner Syndrome gene (7) and of the HIV gene (10) using the two Ag NCs/quencher modules according to (A): (a) Analysis of the Werner Syndrome gene (7) only, 5×10^{-8} M; (b) analysis of the HIV gene (10) only, 31×10^{-8} M; (c) analysis of the two genes, 7 and 10, 5×10^{-8} M and 31×10^{-8} M, respectively. The system is excited at $\lambda = 520$ nm to record the 615 nm luminescence and at $\lambda = 480$ nm to follow the 560 nm luminescence.

analyze the HIV gene, **10**, and three mutants of the gene that include one-base, two-base, and three-base mutations **10a**, **10b**, and **10c**, respectively. Figure 3 shows the fluorescence intensity changes generated by the sensing module upon analyzing the target **10**, curve (a), and the mutants **10a**, **10b**, and **10c**, curves b–d, respectively. As the number of mutations increases, the intensities of the fluorescence changes decrease, consistent with the lower degree of separation of the sensing module. The mutant that includes three-base mismatches (**10c**) yields a very low fluorescence change, implying that the scaffold **9** was not displaced by the mutant.

The successful analysis of the genes associated with the Werner Syndrome and of the HIV gene by the two different luminescent Ag NCs sensing modules allowed the multiplexed analysis of the two genes. Accordingly, the 615 nm luminescent sensing module for analyzing the gene associated with Werner Syndrome was mixed with the 560 nm luminescent sensing module for analyzing the HIV gene, and the composite mixture was applied to analyze the two genes. Figure 4A illustrates the scheme for the multiplexed optical detection of the Werner Syndrome and the HIV genes. Figure 4B, panel a, shows the luminescence spectra changes upon subjecting the system to the gene (**7**) associated with the Werner Syndrome only. The luminescence at 615 nm is intensified (λ_{ex} = 520 nm), with no luminescence change at λ = 560 nm. Exciting the system at λ = 480 nm does not yield any significant luminescence change at λ = 560 nm, nor at 615 nm, indicating that only the gene associated with the Werner Syndrome yields a luminescence change. Similarly, subjecting the mixture composed of the two sensing modules to the HIV gene (**10**) resulted in the luminescence spectra change shown in Figure 4B, panel b. Evidently, only the 560 nm luminescence spectrum is intensified upon analysis of the HIV gene (λ_{ex} = 480 nm), and no significant luminescence change is observed at λ = 615 nm (λ_{ex} = 520 nm, or λ_{ex} = 480 nm), implying that the system responds only to the HIV gene. Finally, the mixture of the sensing modules was subjected to the two genes, **7** and **10**. Figure 4B, panel c, shows that in the presence of the two genes the luminescence of the two Ag NCs is intensified. The 615 nm luminescence is triggered on due to the gene associated with the Werner Syndrome (λ_{ex} = 520 nm), and the luminescence of the 560 nm Ag NCs is triggered on due to the separation of the corresponding sensing module by the HIV gene (λ_{ex} = 480 nm). It should be noted that the excitation spectra of the two different-sized Ag NCs are narrow. As a result, the multiplexed analysis of the two genes is performed by the selective wavelength excitation of the two different-sized Ag NCs. The results indicate the advantages of using the Ag NCs for multiplexed analysis of the genes. The selective narrow-band excitation

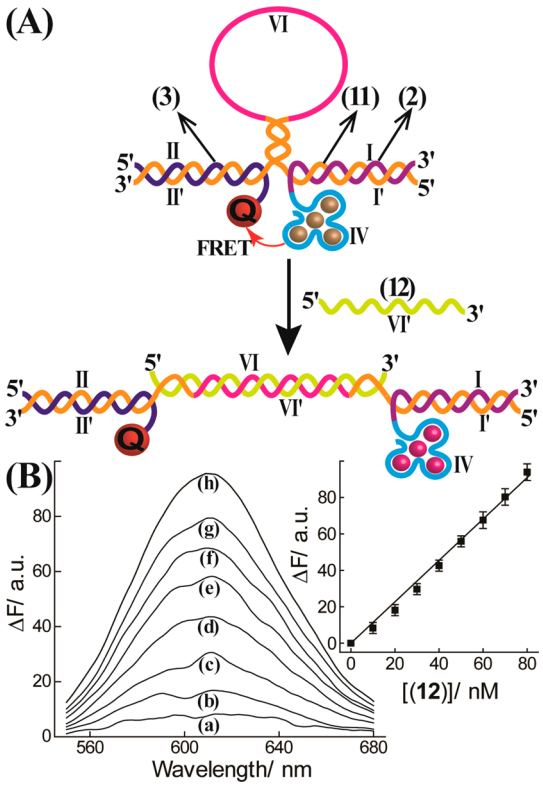

Figure 5. (A) Schematic sensing module for the analysis of the BRCA1 gene (12) using a hairpin DNA scaffold functionalized with a nucleic acid 2-functionalized Ag NCs and a quencher-modified nucleic acid 3. (B) Luminescence spectra changes upon analyzing different concentrations of the BRCA1 gene (12) for a fixed time-interval of 33 min according to (A): (a) 1 × 10^{-8} M, (b) 2 × 10^{-8} M, (c) 3 × 10^{-8} M, (d) 4 × 10^{-8} M, (e) 5 × 10^{-8} M, (f) 6 × 10^{-8} M, (g) 7 × 10^{-8} M, and (h) 8 × 10^{-8} M. Inset: Resulting calibration curve corresponding to the luminescence changes at λ = 615 nm at different concentrations of the HIV gene (12).

of each of the Ag NCs allows the generation of the selective luminescence bands of the two-sized Ag NCs, with no cross-interference between the luminescence bands.

The second sensing platform that implemented a Ag NCs DNA module for the luminescence detection of DNA is shown in Figure 5A. This is exemplified with the sensing of the breast cancer gene, BRCA1. The sensing module consists of the hairpin scaffold **11** to which the nucleic acid **2**, stabilizing the 615 nm luminescent Ag NCs, and the BHQ-modified nucleic acid **3**, were hybridized. The loop domain VI of the hairpin scaffold includes the complementary sequence for the recognition of the BRCA1 gene (**12**). In the hybrid hairpin structure **11**/**2**/**3** the Ag NCs are effectively quenched by BHQ due to the close spatial proximity between the Ag NCs luminophores and the BHQ-quencher unit. In the presence of the BRCA1 gene target **12**, the hairpin structure opens, leading to the spatial separation between the Ag NCs and the BHQ units, resulting in the triggered-"ON" luminescence of the Ag NCs. Figure S6 (Supporting Information) depicts

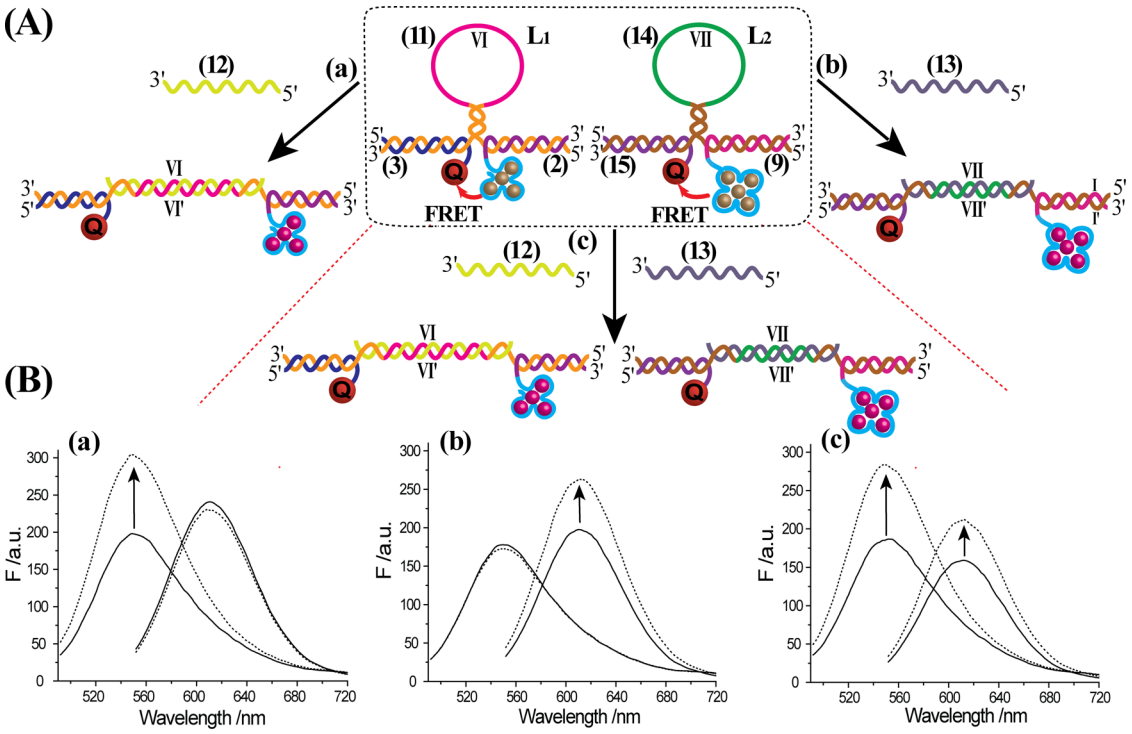

Figure 6. (A) Multiplexed analysis of the BRCA1 gene (12) and of random strand T (13) using the hairpin DNA scaffold composed of the 615 nm luminescent Ag NCs and the 560 nm luminescent Ag NCs. (B) Fluorescence spectra changes upon the multiplexed analysis of the BRCA1 gene (12) and of random strand T (13) using the two Ag NCs/quencher modules according to (A): (a) analysis of random strand T (13), 5×10^{-6} M; (b) analysis of the BRCA1 gene (12), 1×10^{-6} M; (c) analysis of the two analytes (12) and (13), 1×10^{-6} M and 5×10^{-6} M, respectively. The system is excited at λ = 520 nm to record the 615 nm luminescence and at λ = 480 nm to follow the 560 nm luminescence.

the time-dependent luminescence spectra changes upon treatment of the Ag NCs/hairpin sensing module with a fixed concentration of the BRCA1 gene, 8×10^{-8} M. The luminescence spectra changes increase with time, and they level-off after ca. 33 min. The time-dependent changes correspond to the kinetics of opening of the hairpin probe by the analyte DNA (**12**). Figure 5B shows the luminescence spectra changes upon analysis of different concentrations of the BRCA1 gene (**12**) for a fixed time-interval of 33 min, using the sensing module shown in Figure 5A. As the concentration of the BRCA1 gene increases the luminescence changes are intensified, consistent with the higher degree of opening of the hairpin probe, upon elevation of the concentrations of BRCA1 analyte (**12**). The inset of Figure 5B shows the derived calibration curve. The system enabled the detection of the BRCA1 gene with a detection limit that corresponds to 9 nM. We further implemented this sensing module for the multiplexed analysis of genes. Toward this goal, we used two hairpin modules, Figure 6A. One sensing module, L_1, consists of the BRCA1 sensing hairpin, shown in Figure 5, that includes the 615 nm luminescent Ag NCs as probes. The second hairpin module, L_2, is constructed for a random strand T (**13**). The sensing module includes a hairpin strand (**14**) that includes in its loop region the sequence VII that is complementary to the random strand T. The **9**-stabilized 560 nm luminescent NCs and the quencher-functionalized nucleic acid **15** were hybridized with **14** to yield the sensing module for **13**. Figure 6B depicts the multiplexed analysis of the two analytes by the mixture composed of the sensing modules L_1 and L_2. Subjecting the mixture to the random strand T, **13** results in the selective enhancement of the 560 nm luminescent Ag NCs, panel (a). Treatment of the mixture with the BRCA1 gene results in the fluorescence enhancement of the 615 nm luminescent Ag NCs, consistent with the selective opening of hairpin L_1, Figure 6B, panel (b). Treatment of the mixture with both of the analytes BRCA1 (**12**) and T (**13**) results in the increase in the luminescence of both Ag NCs labels, consistent with the multiplexed analysis of the two targets, Figure 6B, panel (c).

CONCLUSIONS

To conclude, the present study has applied different-sized luminescent Ag NCs for the optical detection of genes. Two different sensing platforms for the turn-on detection of genes were introduced, and the use of different-sized Ag NCs for the multiplexed analysis of the genes was demonstrated. A major advantage of the present study, particularly the hairpin sensing module presented in Figures 5 and 6, is reflected by the modularity of the sensing components. The nucleic acid-stabilized Ag NCs and the quencher-modified

nucleic acids may be considered as versatile elements of the module. For analysis of any genes, only the respective hairpin strands need to be programmed. The availability of different nucleic acid-stabilized luminescent metal nanostructures and the sequence-controlled luminescence properties of the metallic NCs pave the grounds for designing new metal NCs-based DNA sensing platforms.

EXPERIMENTAL SECTION

Materials. Ultrapure water from NANOpure Diamond (Barnstead International, Dubuque, IA) was used for all experiments. All other reagents were purchased from Sigma-Aldrich Inc. The DNA strands were purchased from Integrated DNA Technologies Inc. (IDT). All oligonucleotides were HPLC-purified and freeze-dried by the supplier. The oligonucleotides were used as provided and dissolved in an ultrapure water to give stock solutions of 100 μM. The sequences of the oligonucleotides that were used in this study are as follows:

(**1**) 5′-AAC TCT GCT CGA CGG ATT GCA GTA ACG TTA GTC GGA TAA CAG ATC CAT-3′

(**2**) 5′-ACC CGA ACC TGG GCT ACC ACC CTT AAT CCC CAA TCC GTC GAG CAG AGT T-3′

(**3**) 5′-TCC GAC TAA CGT TAC TGC TTT-BHQ-3′

(**4**) 5′-ATG GAT CTG TTA TCC GAC TAA CGT TAC TGC AAT CCG TCG AGC AGA GTT-3′

(**5**) 5′-CAT CTT CAA ATC CAT CTT CTT TTC ATT CCA CTT TGC AGT AAC GTT AGT CGG A-3′

(**6**) 5′-ACC CGA ACC TGG GCT ACC ACC CTT AAT CCC CAA GTG GAA TGA AAA GAA G-3′

(**7**) 5′-AAA GTG GAA TGA AAA GAA GAT GGA TTT GAA GAT G-3′

(**8**) 5′-GAG ACC ATC AAT GAG GAA GCT GCA GAA TGG GAT TGC AGT ACG TTA GTC GGA-3′

(**9**) 5′-CCC TTC CTT CCT TCC AAC CAA CCC ATC CCA TTC TGC AGC TT-3′

(**10**) 5′-ATC CCA TTC TGC AGC TTC CTC ATT GAT GGT CTC-3′

(**10a**) 5′-ATC CCA TTC TAC AGC TTC CTC ATT GAT GGT CTC-3′

(**10b**) 5′-ATC CAA TTC TAC AGC TTC CTC ATT GAT GGT CTC-3′

(**10c**) 5′-ATC CAA TTC TAC AGC TTC CTA ATT GAT GGT CTC-3′

(**11**) 5′-AAC TCT GCT CGA CGG ATT CGT TCT TCC AAC AGC TAT AAA CAG TCC TGG AAG AAC GGC AGT AAC GTT AGT CGG A-3′

(**12**) 5′-CAG GAC TGT TTA TAG CTG TTG GAA G-3′

(**13**) 5′- TCA TTG AAG GAT TTT CCT TGT CAT G-3′

(**14**) 5′- GCT GCA GAA TGG GAT CTT CAT GAC AAG GAA AAT CCT TCA ATG AAG TGG GTC AAT TAT-3′

(**15**) 5′- ATA ATT GAC CCA TTT- BHQ-3′

Synthesis of Fluorescent Ag NCs. The 615 nm luminescent Ag NCs were synthesized by mixing 10 μL of the nucleic acid **2** or **6**, 100 μM, with 20 μL of a phosphate buffer solution, 20 mM, pH = 7.0. To this solution 4 μL of a freshly prepared aqueous solution of $AgNO_3$, 1.5 mM, was added, followed by the vigorous shaking of the solution for 30 s. After 15 min, 4 μL of freshly prepared aqueous solution of $NaBH_4$, 1.5 mM, was added to the solution, followed by vigorous shaking of the mixture for 30 s. The solution was kept in the dark at room temperature and was allowed to react for 12 h. The 560 nm luminescent Ag NCs were synthesized by mixing of the nucleic acid **9** as described above. It should be noted that the Ag NCs reveal fluorescence peaks at 560 and 610 nm, respectively. The fluorescence spectra are, however, not smooth and include fluorescence shoulders. This is due to the inhomogeneity of the sizes of the Ag NCs, as reflected by the ESI-MS analyses (see Table S1, Supporting Information). These features do not affect, however, the sensing process since all Ag NCs are quenched by the BHQ quencher.

Preparation of the Sensing Modules. The analyses were performed in a reaction volume of 150 μL that included phosphate buffer solution, 10 mM, pH = 7.0, HEPES buffer solution, 10 mM, pH = 7.0, and 200 mM $NaNO_3$. The sensing modules: **1**/**2**/**3**, **5**/**6**/**3**, **8**/**9**/**3**, **11**/**2**/**3** were reacted for 30 min and then subjected to the respective targets: **4**, **7**, **10**, and its mutants **12** for different time intervals, at fixed concentrations of the targets, or for a fixed time intervals for variable concentrations of the targets.

Conflict of Interest: The authors declare no competing financial interest.

Supporting Information Available: Time-dependent fluorescence spectra of different sensing modules subjected to the Werner Syndrome gene (**7**), HIV gene (**10**), and BRCA1 gene (**12**). Also, the TEM image of the Ag NCs and the ESI-MS results are provided. This material is available free of charge *via* the Internet at http://pubs.acs.org.

Acknowledgment. This research is supported by the Israel Science Foundation (Grant No. 1083/12). We thank Mr. A. Cecconello for helpful discussions.

REFERENCES AND NOTES

1. Gwinn, E. G.; O'Neill, P.; Guerrero, A. J.; Bouwmeester, D.; Fygenson, D. K. Sequence-Dependent Fluorescence of DNA-Hosted Silver Nanoclusters. *Adv. Mater.* **2008**, *20*, 279–283.
2. Richards, C. I.; Choi, S.; Hsiang, J. C.; Antoku, Y.; Vosch, T.; Bongiorno, A.; Tzeng, Y. L.; Dickson, R. M. Oligonucleotide-Stabilized Ag Nanocluster Fluorophores. *J. Am. Chem. Soc.* **2008**, *130*, 5038–5039.
3. Sharma, J.; Rocha, R. C.; Phipps, M. L.; Yeh, H.; Balatsky, K. A.; Vu, D. M.; Shreve, A. P.; Werner, J. H.; Martinez, J. S. A DNA-Templated Fluorescent Silver Nanocluster with Enhanced Stability. *Nanoscale* **2012**, *4*, 4107–4110.
4. O'Neill, P. R.; Velazquez, L. R.; Dunn, D. G.; Gwinn, E. G.; Fygenson, D. K. Hairpins with Poly-C Loops Stabilize Four Types of Fluorescent Ag_n: DNA. *J. Phys. Chem. C* **2009**, *113*, 4229–4233.
5. Petty, J. T.; Zheng, J.; Hud, N. V.; Dickson, R. M. DNA-Templated Ag Nanocluster Formation. *J. Am. Chem. Soc.* **2004**, *126*, 5207–5212.
6. Vosch, T.; Antoku, Y.; Hsiang, J. C.; Richards, C. I.; Gonzalez, J. I.; Dickson, R. M. Strongly Emissive Individual DNA-Encapsulated Ag Nanoclusters As Single-Molecule Fluorophores. *Proc. Natl. Acad. Sci. U.S.A.* **2007**, *104*, 12616–12621.
7. Ritchie, C. M.; Johnsen, K. R.; Kiser, J. R.; Antoku, Y.; Dickson, R. M.; Petty, J. T. Ag Nanocluster Formation Using a Cytosine Oligonucleotide Template. *J. Phys. Chem. C* **2007**, *111*, 175–181.
8. Petty, J. T.; Fan, C.; Story, S. P.; Sengupta, B.; Sartin, M.; Hsiang, J.-C.; Perry, J. W.; Dickson, R. M. Optically Enhanced, Near-IR, Silver Cluster Emission Altered by Single Base Changes in the DNA Template. *J. Phys. Chem. B* **2011**, *115*, 7996–8003.
9. Petty, J. T.; Fan, C.; Story, S. P.; Sengupta, B.; Iyer, A. S.; Prudowsky, Z.; Dickson, R. M. DNA Encapsulation of 10 Silver Atoms Producing Abright, Modulatable, Near-Infrared-Emitting Cluster. *J. Phys. Chem. Lett.* **2010**, *1*, 2524–2529.
10. Han, B.; Wang, E. DNA-Templated Silver Nanoclusters. *Anal. Bioanal. Chem.* **2012**, *402*, 129–138.
11. Choi, S.; Dickson, R. M.; Yu, J. Developing Luminescent Silver Nanodots for Biological Applications. *Chem. Soc. Rev.* **2012**, *41*, 1867–1891.
12. Latorre, A.; Somoza, Á. DNA-Mediated Silver Nanoclusters: Synthesis, Properties and Applications. *ChemBioChem* **2012**, *13*, 951–958.
13. Su, Y.-T.; Lan, G.-Y.; Chen, W.-Y.; Chang, H.-T. Detection of Copper Ions through Recovery of the Fluorescence of DNA-Templated Copper/Silver Nanoclusters in the Presence of Mercaptopropionic Acid. *Anal. Chem.* **2010**, *82*, 8566–8572.

14. Chen, W.-Y.; Lan, G.-Y.; Chang, H.-T. Use of Fluorescent DNA-Templated Gold/Silver Nanoclusters for the Detection of Sulfide Ions. *Anal. Chem.* **2011**, *83*, 9450–9455.
15. Zhang, L.; Zhu, J.; Guo, S.; Li, T.; Li, J.; Wang, E. Photoinduced Electron Transfer of DNA/Ag Nanoclusters Modulated by G-Quadruplex/Hemin Complex for the Construction of Versatile Biosensors. *J. Am. Chem. Soc.* **2013**, *135*, 2403–2406.
16. Sharma, J.; Yeh, H.-C.; Yoo, H.; Werner, J. H.; Martinez, J. S. Silver Nanocluster Aptamers: *in situ* Generation of Intrinsically Fluorescent Recognition Ligands for Protein Detection. *Chem. Commun.* **2011**, *47*, 2294–2296.
17. Li, J.; Zhong, X.; Zhang, H.; Le, X. C.; Zhu, J.-J. Binding-Induced Fluorescence Turn-On Assay Using Aptamer-Functionalized Silver Nanocluster DNA Probes. *Anal. Chem.* **2012**, *84*, 5170–5174.
18. Liu, X.; Wang, F.; Aizen, R.; Yehezkeli, O.; Willner, I. Graphene Oxide/Nucleic-Acid-Stabilized Silver Nanoclusters: Functional Hybrid Materials for Optical Aptamer Sensing and Multiplexed Analysis of Pathogenic DNAs. *J. Am. Chem. Soc.* **2013**, *135*, 11832–11839.
19. Yeh, H.-C.; Sharma, J.; Han, J. J.; Martinez, J. S.; Werner, J. H. A DNA-Silver Nanocluster Probe That Fluoresces upon Hybridization. *Nano Lett.* **2010**, *10*, 3106–3110.
20. Yeh, H.-C.; Sharma, J.; Shih, I.-M.; Vu, D. M.; Martinez, J. S.; Werner, J. H. A Fluorescence Light-Up Ag Nanocluster Probe That Discriminates Single-Nucleotide Variants by Emission Color. *J. Am. Chem. Soc.* **2012**, *134*, 11550–11558.
21. Shah, P.; Rørvig-Lund, A.; Chaabane, S. B.; Thulstrup, P. W.; Kjaergaard, H. G.; Fron, E.; Hofkens, J.; Yang, S. W.; Vosch, T. Design Aspects of Bright Red Emissive Silver Nanoclusters/DNA Probes for MicroRNA Detection. *ACS Nano* **2012**, *6*, 8803–8814.
22. Liu, X.; Wang, F.; Niazov-Elkan, A.; Guo, W.; Willner, I. Probing Biocatalytic Transformations with Luminescent DNA/Silver Nanoclusters. *Nano Lett.* **2013**, *13*, 309–314.
23. Goldman, E. R.; Clapp, A. R.; Anderson, G. P.; Uyeda, H. T.; Mauro, J. M.; Medintz, I. L.; Mattoussi, H. Multiplexed Toxin Analysis Using Four Colors of Quantum Dot Fluororeagents. *Anal. Chem.* **2004**, *76*, 684–688.
24. Patolsky, F.; Gill, R.; Weizmann, Y.; Mokari, T.; Banin, U.; Willner, I. Lighting-Up the Dynamics of Telomerization and DNA Replication by CdSe-ZnS Quantum Dots. *J. Am. Chem. Soc.* **2003**, *125*, 13918–13919.
25. Freeman, R.; Liu, X.; Willner, I. Chemiluminescent and Chemiluminescence Resonance Energy Transfer (CRET) Detection of DNA, Metal Ions and Aptamer-Substrate Complexes Using Hemin/G-Quadruplexes and CdSe/ZnS Quantum Dots. *J. Am. Chem. Soc.* **2011**, *133*, 11597–11604.
26. Freeman, R.; Liu, X.; Willner, I. Amplified Multiplexed Analysis of DNA by Exonuclease III-Catalyzed Regeneration of the Target DNA in the Presence of Functionalized Semiconductor Quantum Dots. *Nano Lett.* **2011**, *11*, 4456–4461.
27. Liu, X.; Aizen, R.; Freeman, R.; Yehezkeli, O.; Willner, I. Multiplexed Aptasensors and Amplified DNA Sensors Using Functionalized Graphene Oxide: Application for Logic Gate Operation. *ACS Nano* **2012**, *6*, 3553–3563.
28. Sharma, J.; Rocha, R. C.; Phipps, M. L.; Yeh, H.; Balatsky, K. A.; Vu, D. M.; Shreve, A. P.; Werner, J. H.; Martinez, J. S. A DNA-Templated Silver Nanocluster with Enhanced Stability. *Nanoscale* **2012**, *4*, 4107–4110.
29. Chen, L.; Oshima, J. Werner Syndrome. *J. Biomed. Biotechnol.* **2002**, *2*, 46–54.
30. Gray, M. D.; Shen, J.-C.; Kamath-Loeb, A. S.; Blank, A.; Sopher, B. L.; Martin, G. M.; Oshima, J.; Loeb, L. A. The Werner Syndrome Protein Is a DNA Helicase. *Nat. Genet.* **1997**, *17*, 100–103.
31. Huang, S.; Li, B.; Gray, M. D.; Oshima, J.; Mian, I. S.; Campisi, J. The Premature Aging Syndrome Protein, WRN, Is a 3′→5′ Exonuclease. *Nat. Genet.* **1998**, *20*, 114–116.
32. Yu, C. E.; Oshima, J.; Fu, Y. H.; Wijsman, E. M.; Hisama, F.; Alisch, R.; Matthews, S.; Nakura, J.; Miki, T.; Ouais, S.; *et al.* Positional Cloning of the Werner's Syndrome Gene. *Science* **1996**, *272*, 558–562.
33. Lan, G.-Y.; Chen, W.-Y; Chang, H.-T. Controle of Synthesis and Optical Properties of DNA-Templated Silver Nanoclusters by Varying DNA Length and Sequence. *RSC Adv.* **2011**, *1*, 802–807.